

Effects of Silver Addition in Zinc Oxide Nanoparticles on Films of HMSPP/SEBS against *Staphylococcus aureus* and *Escherichia coli* Contamination

Luiz Gustavo Hiroki Komatsu, Giuseppe Montuori Cajado and Duclerc Fernandes Parra

Nuclear and Energy Research Institute, IPEN-CNEN/SP, Av. Prof Lineu Prestes, 2242, Cidade Universitária, CEP 05508-000, São Paulo, SP, Brazil

Abstract: In this research we decided to analyze the addition of silver (Ag°) on zinc oxide (ZnO) utilizing two nanoparticles: the synthesized zinc oxide-doped-silver nanoparticles ($\text{ZnO}/\text{Ag}_{\text{Lab}}$) utilizing the zinc nitrate as metal precursor for ZnO and silver nitrate as metal precursor for Ag° ; and the commercial nanoparticle ZnO/Ag . For the study of application of the nanoparticles, they were processed in the form of films and the polymer utilized was the blend of HMSPP (high melt strength polypropylene) and styrene-ethylene/butadiene-styrene. For the study of nanoparticles, they were submitted to biocide tests against *Staphylococcus aureus* (ATCC 6538) and *Escherichia coli* (ATCC8739) and XRD (X-Ray Diffraction). The XRD analysis results indicated, in both of nanoparticles, with the presence of wurtzite phase of ZnO , being that on the commercial nanoparticles the intensity of peak was higher than that of synthesized one, on other hand, the peaks attributed to Ag° , were more intense in the synthesized nanoparticle.

Key words: Nanoparticles, Biocide Activity, ZnO/Ag .

1. Introduction

The nanoparticles have a biocidal activity as reported in the literature. However, when SARS-COVID-19 in the year 2020 was the most dangerous virus in the world, diverse types of industrial nanoparticles were introduced into the market.

Among the nanoparticles, zinc oxide (ZnO) has a concern due to the its biocide properties, chemical stability and the ZnO has good biocompatibility [1]. ZnO is a very simple nanoparticle to be produced, utilizing diverse methods, among then the sonochemical method [2] this is a simple method to produce nanoparticles with regard to the structure of wurtzite of ZnO . This method was utilized by Gusatti et al. [2] utilizing low temperature and showing a high efficiency to produce nanoparticles.

Another nanoparticle most used for biocidal activity is the metallic silver (Ag). The Ag has good biocidal properties due to the release of the ions of Ag^+ or Ag^0 , which concerns bacteria death [3]. To enhance the biocide properties, the Ag is utilized to dope other nanoparticles, as for example, the doping of the ZnO nanoparticle.

Observing the use of these nanoparticles, we conducted the study of the effects of the Ag addition on ZnO in two steps: the first approach was understanding the effects of the biocide activity against *E. coli* and *S. aureus* and the elements on the nanoparticles by XRD analysis; on the second approach to analyze the biocide effects of the nanoparticles when dispersed on the blend of HMSPP/SEBS. The HMSPP is the high melt strength polypropylene obtained by the gamma irradiation process under acetylene atmosphere, and the SEBS styrene-ethylene/butadiene-styrene thermoplastic elastomer.

Corresponding author: Luiz Gustavo Hiroki Komatsu, Ph.D., polymeric nanocomposites with biocide activity. E-mail: luizkomatsu@gmail.com

2. Experimental Procedure

The chemical materials in this work were utilized without previous treatment. The nanoparticles were named as ZnO/Ag_LAB for the nanoparticle synthesized in the laboratory; and ZnO/Ag_TNS for the nanoparticle purchased from TNS Technology.

2.1 Synthesis of ZnO/Ag_LAB Powder

All solutions were utilized the Mili-Q water, the solution of Zn(NO₃)₂ · H₂O (purchased from LabySynth) was added to the solution of NaOH (purchased from LabySynth) drop by drop under constant stirring, after the solution was heated to the temperature of 75 °C. The suspension was washed and dried, according to an adaptation from the work of Gusatti et al. [2].

For doping the ZnO with silver (Ag), the synthesis utilized was adapted from the Turkevich method [4, 5], the solution of silver nitrate AgNO₃ (purchased from LabySynth) was heated at boiling point, and the sodium citrate was added as reductant agent and the PVP (poly-vinyl-pyrrolidone) (from LabySynth) was incorporated to the solution as a core-shell agent and the synthesized ZnO was added instead to obtain the ZnO doped Ag-ZnO/Ag_LAB.

2.2 Melting Processing

The melting processing was carried out using the extrusion equipment. Firstly, the blend of HMSPP [6, 7] and SEBS was processed in the twin-screw extruder (ThermoHaake Polymer Lab.) [8]. The temperatures utilized were 160 to 210 °C. The mineral oil was added during this process as the plasticizer. In the sequence, in the single screw extrusion (ThermoHaake Polymer Lab.) with temperatures

zones of 160 to 210 °C. The nanoparticles in the powder form were added to the blend of HMSPP/SEBS and extruded to obtain the films of the nanocomposites. The average film thickness was 0.07 and 0.09 mm.

2.3 XRD (X-Ray Diffraction)

XRD measurements were carried out in the reflection mode on a Rigaku diffractometer Mini Flex II (Tokyo, Japan) operated at 30 kV voltage and a current of 15 mA with CuK θ radiation ($\lambda = 1,541841 \text{ \AA}$).

2.4 Biocide Tests

This test was carried out to evaluate the biocidal activity of the nanoparticles. The bacteria used for this test were the *Staphylococcus aureus* ATCC 6538 and *Escherichia coli* ATCC8739.

The standard used for testing the nanoparticles was the INCQS 65.3240.016—Method for Evaluation of Bactericide and Fungicide Activity of Substances and Sanitizing Preservatives.

The standard used for testing the films with the nanoparticles was the JIS 2801—Japanese International Standard—Test for Antimicrobial Activity of Plastics.

3. Results

In Table 1, halo biocide tests for each nanoparticle on the microorganisms are reported. *Staphylococcus aureus* ATCC 6538 and *Escherichia coli* ATCC8739 microorganisms were utilized for the test owing to the large spectrum of contamination of these microorganisms and Fig. 1 reports the agar plate resulted for the halo of inhibition measurement.

Table 1 Measurement of inhibition halo diameter on the biocidal test of the nanoparticles, following the INCQS 65.3240.016 norm.

Microorganisms	ZnO	Sample/halo (mm)	
		ZnO/Ag_LAB	ZnO/Ag_TNS
<i>Staphylococcus aureus</i> ATCC6538	2	3	2
<i>Escherichia coli</i> ATCC8739	2	4	1

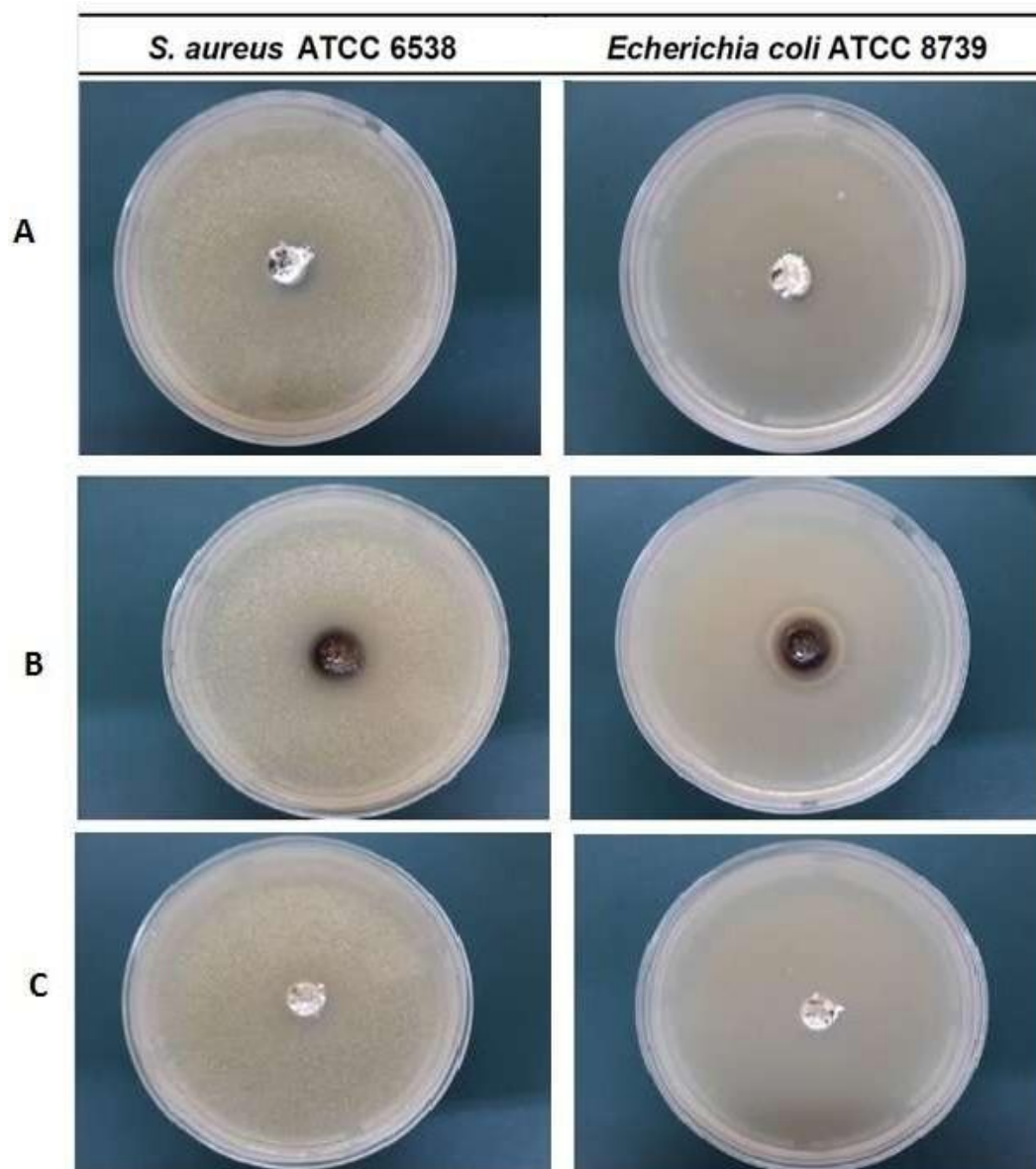


Fig. 1 Nanoparticles submitted to biocide analysis against the *S. aureus* and *E. coli*; following the INCQS norm: ZnO (A); ZnO/Ag_LAB (B) and ZnO/Ag_TNS (C).

The biocide activity was observed for all of the nanoparticles. Observing each nanoparticle in Table 1 and Fig. 1, the biocide activity in the ZnO nanoparticles was attributed to the possibility of Zn^{2+} ions present on the surface of the nanoparticles. According to the literature [9] these ions interact with the cell bacteria causing the death. Another mechanism, highlighted in the literature, describes the effect of the morphology for physic deformation of the cell [10] and the generation of three types of ROS ($\cdot OH$, 1O_2 , $O_2^{\cdot -}$), causing higher oxidative stress on

biological systems, and causing the cell death [5].

In the case of ZnO/Ag_LAB and ZnO/Ag_TNS, further the presence and action of ZnO nanoparticles, the presence of silver increased the biocide activity. The silver has diverse types and/or shapes, among them the Ag^0 , which is the form that has possibilities of the biocide effect thus in UV light and dark ambient.

Observing the results, the ZnO/Ag_LAB has a halo diameter more pronounced than ZnO/Ag_TNS for both microorganisms.

To corroborate this experimental observation, on the biocide tests, we analyzed by Inductively Coupled Plasma Optical Emission Spectrometry (ICP-OES) the concentration of each element Zn or Ag. The ZnO/Ag_LAB has concentration of 205 mg/L of Ag and 38 mg/L of Zn and ZnO/Ag_TNS has concentration of 2.2 mg/L of Ag and 714 mg/L of Zn. With this result, in part, it is possible to affirm that biocidal activity on ZnO/Ag_LAB is increased due to the Ag addition and in the ZnO/Ag_TNS the biocidal activity was mainly correlated to the presence of ZnO.

The literature cites [12], the ions of Zn^{2+} and/or Ag^+ ; Ag^0 can be released from each respective nanoparticle. Each ion has a different target for different types of protein cells and in this form inactivates. The Ag^+ , Ag^0 can combine with the chloride ions and precipitate into silver chloride, inhibiting cell respiration. The zinc can link with the membranes changing the permeability to the cells, while the Ag^+ ions can inhibit the DNA (deoxyribonucleic acid) replication, as cited in the literature [12], and the silver activity is related to the fact of the silver bonded with the proteins, affects the respiration process destroying the external membrane with the cell death.

In addition, on Dynamic Light Scattering (DLS) and zeta potential, the average size of the nanoparticles was observed: ZnO = 800 nm and -4.77 mV of zeta potential; ZnO/Ag_LAB = 75.85 nm and -21.2 mV of zeta potential; ZnO/Ag_TNS = 1,786 nm and -10.7 mV of zeta potential. With this data, it is possible to affirm on ZnO/Ag_TNS, the incorporation of the silver on the ZnO is carried out utilizing a mechanical method due to the comparison between particle size of the ZnO/Ag_TNS and ZnO/Ag_Lab; and by the observation of the zeta potential, the experimental value of potential zeta of ZnO/Ag_LAB was nearby the -40 mV indicating in this form, this nanoparticle has intense charge repulsion between the nanoparticles conduction to a more stable particle, preventing the agglomeration. Through the literature cited [13], it is possible to revert the agglomeration

state, however if an additional entropy, such as sonication, homogenization or ion exchange (H^+) is added to the synthesis process, this observation of the literature confirms the fact that synthesized ZnO used on ZnO/Ag_LAB allows a diminution of the size average of nanoparticle doped with silver size below 100 nm.

To analyze other aspects from the nanoparticles, the XRD was carried out in the powder of the nanoparticles and with the diffractogram shown in Fig. 2, it is possible to identify each ion on the nanoparticle.

The crystalline structure of each nanoparticle was observed and confirmed in XRD analysis. The identified peaks in Fig. 2 were: $2\theta = 10.75^\circ$; 13.98° ; 15.26° ; 18.09° ; 19.58° (Ag Metallic); 23.10° ; 23.98° (ZnO); 28.67° (ZnO/Ag); 30.33° ; 31.12° ; 31.81° ; 35.34° ; 36.51° (ZnO wurtzite); 38.46° (Ag crystalline phase); 39.83° ; 40.99° ; 44.52° (Ag crystalline phase); 46.33° (ZnO wurtzite); 49.91° ; 54.31° (Silver nitrate residue); 55.68° (ZnO wurtzite); 56.76° (Silver nitrate residue); 59.99° ; 64.80° ; 77.62° (ZnO wurtzite). The diffraction peaks confirm the presence of ZnO and the Ag on the nanoparticles, the peaks referring to the Ag are more stable and visible when compared to the other nanoparticle ZnO/Ag_Lab, this fact occurs due to the process of core-shell with PVP that stabilized the growth of the particle during the process of synthesis [14-19]. In both nanoparticles, it was identified that the residue of nitrate (NO_3^-) is utilized in the process of doping of ZnO and the synthesis of ZnO. In the case of ZnO/Ag_LAB, the intensity of the peak is weak when compared to the ZnO/Ag_TNS, indicating the fact that the nitrate is almost enough consumed during the process of synthesis.

The peaks of ZnO indicate the presence of form of wurtzite zinc oxide. This structure has a hexagonal structure, as simply described as some alternating planes composed of tetrahedral coordinated O^{2-} and Zn^{2+} [20].

In parallel, the material has the influence of silver the presence of particles of metallic Ag. Another reason

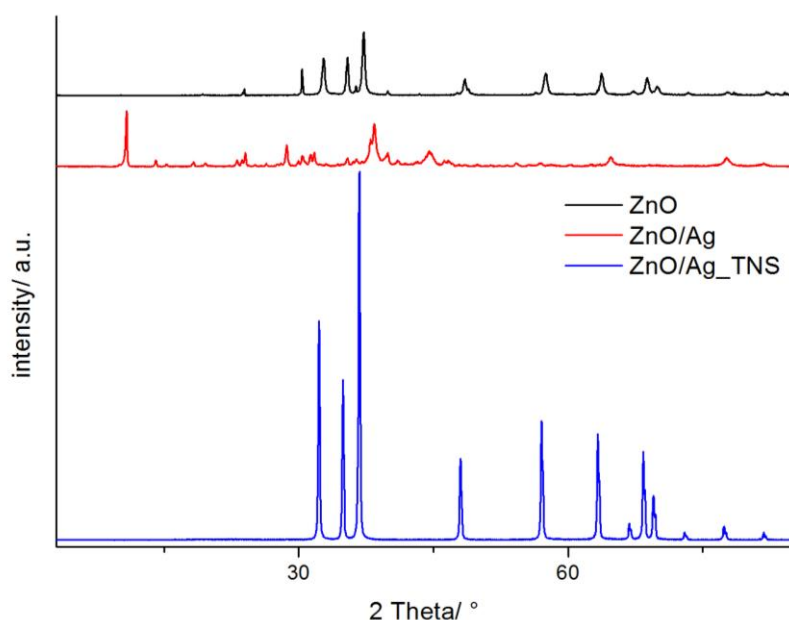


Fig. 2 XRD diffractogram of the nanoparticles of ZnO/Ag_LAB, ZnO/Ag_TNS and ZnO.

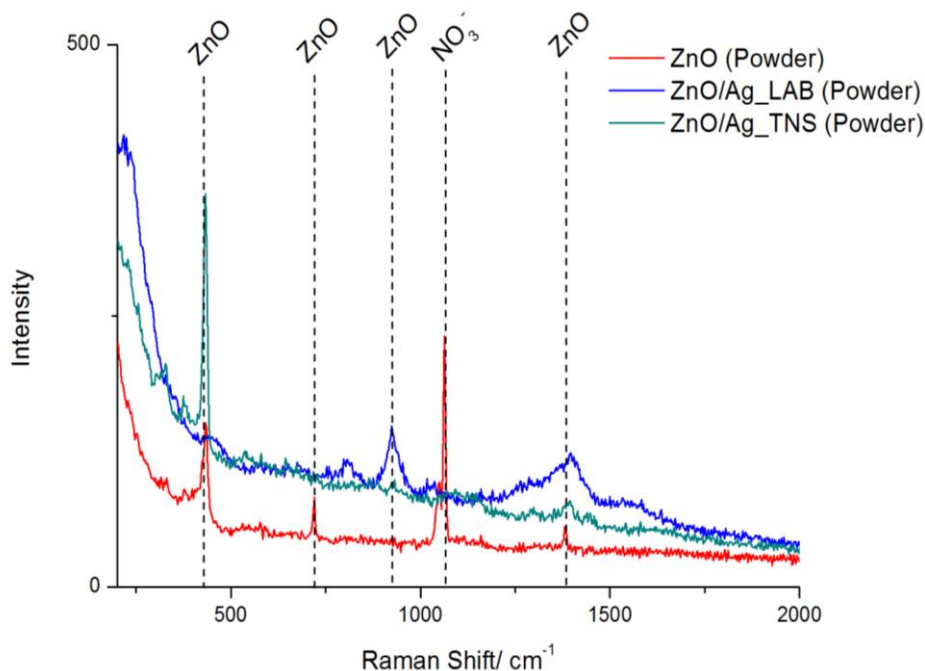


Fig. 3 Raman Confocal carried out on the nanoparticles of ZnO, ZnO/Ag_LAB and ZnO/Ag_TNS.

is the fact that the ZnO acts as Ag carrier in the case of ZnO/Ag_LAB. The core shell provided by PVP on Ag^+ reduced from AgNO_3 , controlled the growth of Ag nanoparticles, and provided a chemical ligament with the ZnO.

The Raman Confocal was utilized to better understand and corroborate the characteristics of the

nanoparticles; the diffractogram of the nanoparticles was represented in Fig. 3.

The experimental wave numbers were observed on the nanoparticles and represented in Fig. 3, and the peaks of ZnO identified by 440 cm^{-1} , 724 cm^{-1} , 927 cm^{-1} , $1,069 \text{ cm}^{-1}$, $1,385 \text{ cm}^{-1}$, $1,405 \text{ cm}^{-1}$ were attributed to the formation of ZnO nanocrystals in the format of

Wurtzite [21, 22], corroborating with the results observed in the XRD diffractogram.

The intense peak of 1038 cm^{-1} in the ZnO was associated to free anion of NO_3^- [24]. This peak can be related with the residual NO_3^- from the synthesis of ZnO and Ag; and can be related to a residual from the process of washing of the nanoparticles.

The peaks of 808 cm^{-1} , $1,149\text{ cm}^{-1}$, $1,334\text{ cm}^{-1}$, $1,459\text{ cm}^{-1}$ were observed on the ZnO/Ag_LAB and in the ZnO/Ag_TNS, and were attributed to the presence of the silver [24].

Analyzing the nanoparticles isolated, it is possible to conclude both nanoparticles have a biocide effect against the microorganisms, however, when each particle is melt processed with other polymers, like polyolefin, there exists the possibility of alteration of its properties due to the higher temperature, high shear rate, during the melting processing.

To study the effects of melting processing on the nanoparticles, the blend of HMSPP/SEBS was obtained and doped with concentrations of the nanoparticles, as described on the methodology, and melt processed in thin film form for study.

After the process, the samples were cleaned with alcohol ethylic and submitted to the biocide assay following the JIS norm and the results are shown in Table 2.

The bactericidal efficacy of the nanoparticles on the films of the blend of HMSPP/SEBS was evaluated by observing the logarithmic reduction after 24 h of

incubation and the count of bacteria cells, as observed in Table 2. Considering the standard efficiency defined in the JIS norm, all samples showed biocide activity, with exception of the film with ZnO/Ag_TNS against the gram-negative bacteria *E. coli*.

Considering the mechanisms observed in the analysis of biocide effects on the nanoparticles, the films containing ZnO/Ag_TNS were possible to decrease the bacteria growth in the case of *S. aureus*, by observing the results of bacteria counting after 24 h, this fact can be correlated to the fact that the presence of ZnO is in major evidence than Ag, as observed in XRD and the *S. aureus* is more sensitive for biocide nanoparticles, in this case of ZnO/Ag.

On other hands, the films of ZnO/Ag_LAB were possible to decrease the bacteria counting. In this part, it is possible to observe the similarity between the logarithmic reduction in both the nanoparticles, despite counting cells of bacteria after 24 h in the films with ZnO/Ag_TNS being higher than the ZnO/Ag_LAB.

Observing this, it is possible to affirm that mechanism of interaction of the bacteria with the nanoparticles/film has some changes. It is possible, during the processing in twin-screw extruder, the nanoparticles are exposed to high temperatures, high shear rate, and other side effects. In those cases, the nanoparticles had a loss of their properties due to the oxidation process of them. In this context, for the gram-negative bacteria, *E. coli*, it is possible to affirm the films of nanoparticles ZnO/Ag_TNS have a loss of properties during the

Table 2 Biocide tests following the JIZ norm on the films of blend of HMSPP/SEBS with the nanoparticles of ZnO, ZnO/Ag_LAB and ZnO/Ag_TNS on the bacteria *S. aureus* and *E. coli*.

Samples films	Bacteria			Bacteria		
	Counting in zero time <i>S. aureus</i> ATCC 6538P	Counting after 24 h <i>S. aureus</i> ATCC 6538P	Logarithmic reduction	counting in zero time zero <i>E. coli</i> ATCC 8739	counting after 24 h <i>E. coli</i> ATCC 8739	Logarithmic reduction
1% ZnO	2.3×10^5	2.7×10^4	0.93	2.6×10^5	2.0×10^5	0.11
0.3% ZnO	2.3×10^5	2.1×10^4	1.04	2.6×10^5	2.1×10^5	0.09
1% ZnO/Ag_Lab	2.3×10^5	1.2×10^2	3.28	2.6×10^5	1.5×10^2	3.23
0.3% ZnO/Ag_Lab	2.3×10^5	7.6×10^2	2.48	2.6×10^5	5.6×10	3.66
1% ZnO/Ag_TNS	2.3×10^5	3.0×10	3.88	2.6×10^5	1.9×10^5	0.13
0.3% ZnO/Ag_TNS	2.3×10^5	3.2×10^2	2.85	2.6×10^5	1.7×10^5	0.18

process, in this form conducting to a lower number of counting cells and logarithmic reduction values when compared to the ZnO/Ag_LAB. Another reason for loss of the properties of the nanoparticles, is the

dispersion of the nanoparticles on the surface of the film. To corroborate this observation, the films were analyzed on the Raman confocal represented in Figs. 4A and 4B.

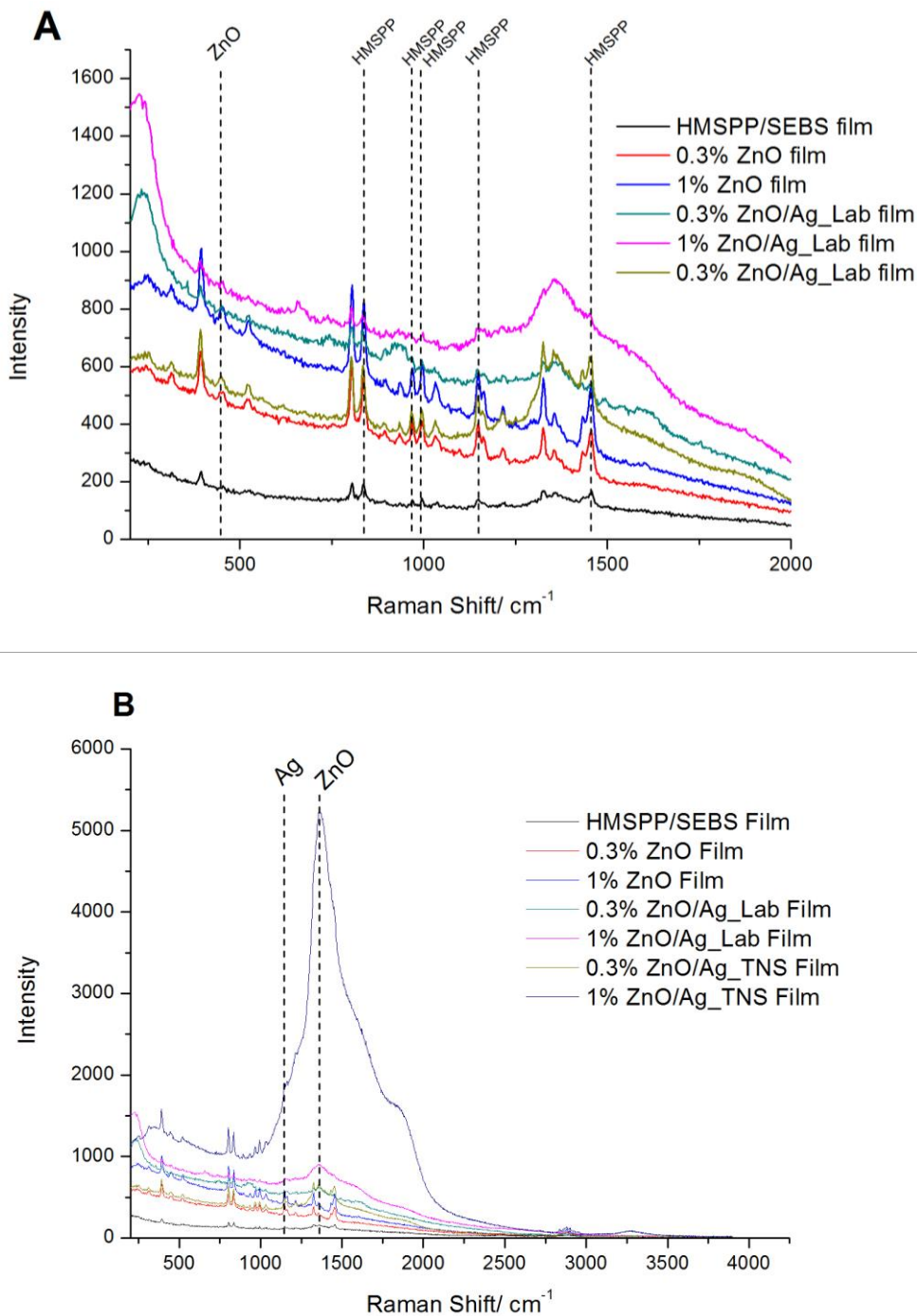


Fig. 4 Raman Confocal on the films of blend HMSPP/SEBS with the nanoparticles of ZnO, ZnO/Ag_LAB and ZnO/Ag_TNS. The figure 4 (A) is referred to all concentrations and the figure 4(b) is referred to an comparison to the film of 1% of ZnO/Ag_TNS

The experimental peaks identified in Figs. 4A and 4B, which were: 841 cm^{-1} , 998 cm^{-1} , 970 cm^{-1} , 1,152 cm^{-1} , 1,324 cm^{-1} , 1,432 cm^{-1} , 1,457 cm^{-1} , attributed to the HMSPP polymer. The peak of ZnO of 440 cm^{-1} was identified in the films with the nanoparticles. The peaks referred to the nanoparticles also appear in Fig. 3. It is interesting to observe in Fig. 4B that in the film of ZnO/Ag_TNS, the peak referred to ZnO, 1,369 cm^{-1} ; and Ag, 1,149 cm^{-1} increased in such way that almost hide the other peaks. In observation of the experimental peaks, the presence of the ZnO is evident in the case of ZnO/Ag_TNS, however, there exists the probability that the dispersion of the particle on the surface is compromised, confirming the hypothesis of the synthesis of the ZnO/Ag_TNS was carried by mechanical process, because the peak of ZnO is strong when compared to the others, this fact can be correlated to the biocide activity and the melt processing. The melt processing can separate the ZnO and Ag by shear rate and the dispersion in the film changed the biocidal activity. Otherwise, in the ZnO/Ag_LAB, the molecules of ZnO and Ag were intimately formed, and in this form have a better dispersion in the surface of the film.

4. Conclusions

We have studied the addition of the silver on the ZnO and ZnO/Ag nanoparticles by analyzing the biocidal activity before and after melting processing. The enhancement of biocidal activity because of silver addition was observed. For ZnO/Ag_TNS, a fact was verified that a mechanical addition can provide a biocide activity on ZnO, however, this method of synthesis does not maintain stable the biocide properties of the nanoparticles after melting processing. On ZnO/Ag_LAB, a stable nanoparticle was found with biocide activity before and after melting processing.

Acknowledgements

The authors thanks CNPq, Capes/PROEX (88882.333460/2019-1), CNEN (01341.011047/2021-

33) for the grants, ControlBIO for the biocide tests. LQSN group from Chemistry Institute—USP, for the analysis and scientific support.

References

- [1] Rojas, K., Canales, D., Amigo, N., Montoille, L., Cament, A., Rivas, L. M., Gil-Castell, O., Reyes, P., Ulloa, M. T., Ribes-Greus, A., and Zapata, P. A. 2019. "Effective Antimicrobial Materials Based on Low-Density Polyethylene (LDPE) with Zinc Oxide (ZnO) Nanoparticles." *Composites Part B* 172: 173-8.
- [2] Gusatti, M., Rosario, J. A., Barroso, G. S., Campos, C. E. M., Riella, H. G., and Kunhen, N. C. 2009. "Synthesis of ZnO Nanostructures in Low Reaction Temperature." *Chemical Engineering Transitions* 17: 1017-26.
- [3] Alarcon, M. I., Griffith, M., and Udekwo, K. I. 2015. *Silver Nanoparticle Applications in the Fabrication and Design of Medical and Biosensing Devices*. Switzerland: Springer International Publishing. ISBN 978-3-319-11262-6.
- [4] Oliveira, G. M., Costa, L. M. M., Carvalho, A. J. F., Basmaji, P., and Pessan, L. A. 2011. "Novel LDPE/EVA Nanocomposites with Silver/Titanium Dioxide Particles for Biomedical Applications." *Journal of Materials Science and Engineering B* 1: 516-22.
- [5] Turkevich, J., Stevenson, P. C., and Hillier, J. 1951. "A Study of the Nucleation and Growth Processes in the Synthesis of Colloidal Gold." *Discussions of the Faraday Society* 11: 55-75.
- [6] Lugão, A. B., Otaguro, H., Parra, D. F., Yoshinaga, A., Lima, L. F. C. P., Artel, B. W. H., and Liberman, S. 2007. "Review on the Production Process and Uses of Controlled Rheology Polypropylene-Gama Radiation versus Electron Beam Processing." *Radiation Physics and Chemistry* 76: 1688-90.
- [7] Lugao, A. B., Noda, L., Cardoso, E. C. L., Hustzler, B., Tokumoto, S., and Mendes, A. N. F. 2002. "Temperature Rising Elution Fractionation, Infrared and Rheology Study on Gama Irradiated HMSPP." *Radiation Physics and Chemistry* 63: 509-12.
- [8] Komatsu, L. G. H., Oliani, W. L., Oliveira, C. B., Rangari, V. K., and Parra, D. F. 2020. "Application of ZnO an ZnO-Doped-Ag in Polymeric Blend of HMSPP/SEBS for Biocide Activity." In *Characterization of Minerals, Metals, and Materials (The Minerals, Metals & Materials Series)*. Cham: Springer. doi: https://doi.org/10.1007/978-3-00-36628-5_41.
- [9] Li, Y., Zhang, W., Niu, J., and Chen, Y. 2012. "Mechanism of Photogenerated Reactive Oxygen Species and Correlation with the Antibacterial Properties of Engineered Metal-Oxidative Nanoparticles." *ACS Nano* 6 (6): 5164-73.

116 **Effects of Silver Addition in Zinc Oxide Nanoparticles on Films of HMSPP/SEBS against *Staphylococcus aureus* and *Escherichia coli* Contamination**

- [10] Simoes, D. N., Pittol, M., Tomacheski, D., Ribeiro, V. F., and Santana, R. M. C. "Thermoplastic Elastomers Containing Zinc Oxide as Antimicrobial Additive under Thermal Accelerated Ageing." *Materials Research* 20: 325-30. <http://dx.doi.org/10.1590/1980-5373-MR-2016-0790>.
- [11] Kulshreshtha, N. M., Jadhav, I., Dixit, M., Sinha, N., Shrivastava, D., and Bisen, P. S. 2017. *Nanostructures as Antimicrobial Therapy*. Netherlands: Elsevier.
- [12] Khan, S. T., and Al-Khedahairy, A. A. 2017. "Metals and Metal Oxides: Important Nanomaterials with Antimicrobial Activity." In *Antimicrobial Nanoarchitectonics: From Synthesis to Applications*. Netherlands: Elsevier.
- [13] Berg, J. M., Romoser, A., Banerjee, N., Zebda, R., and Sayes, C. M. 2009. "The Relationship between pH and Zeta Potential of ~30nm Metal Oxide Nanoparticles Suspensions Relevant to *in Vitro* Toxicological Evaluations." *Nanotoxicology* 3 (4): 276-83.
- [14] Abutalib, M. M., and Rajeh, A. 2020. "Influence of ZnO/Ag Nanoparticles Doping on the Structural, Thermal, Optical and Electrical Properties of PAM/PEOI Composite." *Physica B: Physics of Condensed Matter* 578: 411-9.
- [15] Abedini, A., Saraji, M., Bakar, A. A. A., Menon, P. S., and Shaari, S. 2017. "Gamma-Radiation-Assisted Synthesis of Luminescent ZnO/Ag Heterostructure Core-Shell Nanocomposites." *Plasmonics* 13: 771-8.
- [16] Gugur, E., Oluyamo, S. S., Adetuyi, A. O., Omotunde, O. I., and Okoronkwo, A. E. 2020. "Green Synthesis of Zinc Oxide Nanoparticles and Zinc Oxide-Silver, Zinc Oxide-Copper Nanocomposites Using *Bridelia ferruginea* as Biotemplate." *SN Applied Sciences* 2: 911-23. <https://doi.org/10.1007/S42452-020-2269-3>.
- [17] Pascariu, P., Cojocar, C., Samoila, P., Airinei, A., Oлару, N., Rusu, D., Rosca, I., and Suche, M. 2020. "Photocatalytic and Antimicrobial Activity of Electronspon ZnO:Ag Nanostructures." *Journal of Alloys and Compounds* 834: 144-55.
- [18] Abutalib, M. M., and Rajeh, A. 2020. "Influence of ZnO/Ag Nanoparticles Doping on the Structural, Thermal, Optical and Electrical Properties of PAM/PEO Composite." *Physica B* 578: 411-796.
- [19] Ahmed, D. S., Mohamed, M. R., and Mohammed, M. K. A. 2020. "Synthesis of Multi-walled Carbon Nanotubes Decorated with ZnO/Ag Nanoparticles by Co-precipitation Method." *Nanoscience & Nanotechnology-Asia* 10: 127-33.
- [20] Wang, Z. L. 2004. "Zinc Oxide Nanostructures: Growth, Properties and Applications." *Journal of physics Condensed Matter* 16: 829-58.
- [21] Wang, Y., Ruan, W., Zhang, J., Yang, B., Xu, W., Zhao, B., and Lombardi, J. R. 2009. "Direct Observation of Surface-Enhanced Raman Scattering in ZnO Nanocrystals." *Journal of Raman Spectroscopy* 40: 1072-7.
- [22] Sirelkhatim, A., Mahmud, S., Seeni, A., Kaus, N. H. M., Ann, L. C., Bakhori, S. K. M., Hasan, H., and Mohamad, D. 2015. "Review on Zinc Oxide Nanoparticles: Antibacterial Activity and Toxicity Mechanism." *Nano-Micro Letters* 7: 219-42.
- [23] Kim, J. H., Min, B. R., Kim, C. K., Won, J., and Kang, Y. S. 2002. "Spectroscopic Interpretation of Silver Ion complexation with Propylene in Silver Polymer Electrolytes." *Journal Physical Chemistry B* 106: 2786-90.
- [24] Al-Shalalfeh, M. M., Onawole, A. T., Saleh, T. A., and Al-Saadi, A. A. 2017. "Spherical Silver Nanoparticles as Substrates in Surface-Enhanced Raman Spectroscopy for Enhanced Characterization of Ketoconazole." *Materials Science and Engineering C* 76: 356-64.